Journal de Théorie des Nombres de Bordeaux

anciennement Séminaire de Théorie des Nombres de Bordeaux

James DOLAN et Oleg KARPENKOV

Lattice angles of lattice polygons

Tome 37, nº 3 (2025), p. 873-896.

https://doi.org/10.5802/jtnb.1345

e-ISSN : 2118-8572

Journal de Théorie des Nombres de Bordeaux **37** (2025), 873–896

Lattice angles of lattice polygons

par James DOLAN et Oleg KARPENKOV

Résumé. Cet article est consacré à l'analogue, en théorie des réseaux, de la formule classique de la somme des angles intérieurs d'un polygone. Bien que, en 2008, la première formule donnant des conditions sur les fractions continues géométriques pour les angles réseaux des triangles a été obtenue, le cas des n-gones pour $n > 3$ demeurait non résolu. Dans cet article, nous proposons une solution complète pour tout entier n. Les principaux résultats reposent sur les avancées récentes en géométrie des fractions continues.

Abstract. This paper is dedicated to a lattice analog to the classical "sum of interior angles of a polygon theorem". In 2008, the first formula expressing conditions on the geometric continued fractions for lattice angles of triangles was derived, while the cases of n-gons for $n > 3$ remained unresolved. In this paper, we provide the complete solution for all integer n. The main results are based on recent advances in geometry of continued fractions.

1. Introduction

The *sum of interior angles of a polygon theorem* in Euclidean geometry states that the sum of all interior angles of an n-gon equals $(n-2)\pi$; for any sequence of n non-zero angles smaller than π, altogether summing to $(n-2)\pi$, there exists a convex n-gon with these angles. In this paper, we study the lattice analog of this theorem. The integer analog for the Euclidean measure of angles are the LLS-sequences (see Subsection 2.4 for necessary definitions). We provide a solution to the following problem.

Problem 1 (IKEA problem)**.** Classify all n-tuples of LLS-sequences for the angles that form integer n-gons.

(This problem is equivalent to the classification problem of the admissible collections of toric singularities for a toric surface with a fixed Euler characteristics, for further details see e.g. in [18, Chapter 17]).

We develop criteria for given lattice angles to be the angles of some convex lattice polygons (Theorem 3.3 and Theorem 3.8). Without loss of generality, we restrict ourselves to the case of the integer lattice whose group of symmetries is the group of affine integer lattice preserving transformations

Manuscrit reçu le 21 juin 2024, révisé le 28 novembre 2024, accepté le 12 janvier 2025.

2020 *Mathematics Subject Classification.* 11A55, 11H06, 52C05.

Mots-clefs. lattice geometry, integer trigonometry, continued fractions, lattice polygons, IKEA problem.

$\mathrm{Aff}(2, \mathbb{Z})$. This group is a semidirect product of the group of multiplication by $\mathrm{GL}(2, \mathbb{Z})$ matrices and the group of translations on vectors with integer coordinates. As a by-product, we obtain a new integer generalisation of the angle-side-angle rule for triangle congruence (Proposition 2.23).

The case of triangles was answered in 2008 in [14]. The proof was given in terms of values of long continued fractions geometrically defined by rational angles (for further details on integer geometry we refer to [2, 16, 18]). These fractions are closely related to the theory of integer trigonometric functions developed in [14, 15]. In this paper, we cover all of the remaining cases of n-gons (i.e. $n > 3$), which completes the solution of Problem 1.

There are numerous publications related to various classifications of convex lattice polygons and their frequencies. In particular, the statistics of integral convex polygons were studied in [1] by V. Arnold and in [3] by I. Bárány and A.M. Vershik. In [6, 30] (and later developed in [9]) the authors study the notion of lattice sizes of lattice polygons. H. Lenstra used lattice width of lattice polytopes in order to solve the feasibility question of integer linear programming [25] (for the two-dimensional case see [7, 8]). Recently in [10] M. Henk, S. Kuhlmann and R Weismantel studied lattice width of lattice-free polyhedra. In [29] R. Morrison and A.K. Tewari classified convex lattice polygons with all lattice point visible. Gauss–Kuzmin statistics of such polygons were studied by M. Kontsevich [24] and further related to hyperbolic geometry by the second author in [13].

The relation on the angles in convex polyhedra defines the global relations to cusp singularities in toric varieties [14, 32] and their interplay with rigidity theory [28]. Collection of angles in the polygons impact the values of coefficients in Earhart polynomials, see e.g. in [4].

This paper is organised as follows. In Section 2, we give all necessary definitions on continued fractions, sails of angles, and chord curvatures of broken lines. We also adapt the generalised angle-side-angle rule for lattice geometry. We formulate the main results on the relations between the angles of lattice n-gons in Section 3. Further in Section 4, we introduce additional notions and definitions that are required for the proofs and prove some auxiliary statements. Finally in Section 5, we complete the proofs of main results. We conclude this paper in Section 6 with a short discussion on the IKEA problem in the multidimensional case, which is still open.

2. Preliminary definitions and formulation of the main statements

In this section we give basic definitions of lattice geometry, continuants and continued fractions. We discuss locally convex broken lines and introduce the angle-curvatures sequences classifying them. Finally we present a new integer angle-side-curvature-angle rule.

2.1. The monoid of finite integer sequences under concatenation. Denote the set of all integer sequences by

$$\mathbb{Z}^* = \bigcup_{n=0}^{\infty} \mathbb{Z}^n,$$

where $\mathbb{Z}^0 = \{\epsilon\}$ represents the empty sequence $\epsilon = ()$. There is the following natural operation of concatenation acting on $\mathbb{Z}^*$. Consider

$$X = (x_1, \ldots, x_n) \in \mathbb{Z}^* \quad \text{and} \quad Y = (y_1, \ldots, y_m) \in \mathbb{Z}^*.$$

Then the *concatenation* $X \circ Y$ is the sequence

$$X \circ Y = (x_1, \ldots, x_n, y_1, \ldots, y_m).$$

We have that $(\mathbb{Z}^*, \circ)$ is a monoid.

2.2. Continuant and continued fractions. Let us recall the classic notion of continued fractions.

Definition 2.1. Let $\alpha \in \mathbb{R} \cup \{\infty\}$ and $a_0, \ldots, a_n$ be real numbers satisfying the following equation

$$\alpha = a_0 + \cfrac{1}{a_1 + \cfrac{1}{a_2 + \cfrac{1}{\ddots + \cfrac{1}{a_n}}}}$$

Then we say that the expression in the right-hand side of the equality is a *continued fraction expansion* of α; we denoted this by $[a_0; a_1 : \ldots : a_n]$. We say that $n+1$ is the length of the continued fraction and that $a_0, \ldots, a_n$ are the *elements* of this continued fraction.

Remark 2.2. While evaluating these expressions on the right hand side, we might get 0 intermediate values. Here are the following simple three rules to deal with them

$$\frac{1}{0} = \infty, \qquad a + \infty = \infty, \qquad \frac{1}{\infty} = 0.$$

The following function is closely related to the notion of the continued fraction.

Definition 2.3. The *continuant function* $K : \mathbb{Z}^* \to \mathbb{Z}$ is defined iteratively as follows:

$$K(\epsilon) = 1, \qquad K(x_1) = x_1,$$
$$K(x_1, \ldots, x_n) = x_n K(x_1, \ldots, x_{n-1}) + K(x_1, \ldots, x_{n-2}), \quad \text{for } n \geq 2.$$

Remark 2.4. Continuants and continued fractions are linked by the following formula.

$$[a_0; a_1 : \ldots : a_n] = \frac{K(a_0, a_1, \ldots, a_n)}{K(a_1, \ldots, a_n)}.$$

For more information on theory of continued fractions see [18, 21].

2.3. Definitions of integer geometry. We say that a point/vector in $\mathbb{R}^2$ is *integer* if its coordinates are integer. A straight line is said to be integer if it contains at least two distinct integer points. A ray is said to be integer if its vertex is integer, and the straight line containing the ray is integer. An angle (i.e. the union of two rays with the common vertex) is said to be *rational* if the rays defining it are integer and if they do not belong to the same line (here we use the term "rational" in order to indicate that the slopes of the rays of such angle are rational numbers).

Let us collect the following invariants of lattice geometry.

Definition 2.5.

- The *integer length* of an integer segment AB is the number of connected components in $AB \setminus \mathbb{Z}^2$. Denote it by $\mathrm{l}\ell(AB)$.
- Let AB and AC be two integer segments, then the value $\det(AB, AC)$ is invariant under the action of $\mathrm{Aff}(2, \mathbb{Z})$. It is called *oriented integer area* of the triangle $\triangle BAC$. Here the absolute value of $\det(AB, AC)$ is called the *integer area* of $\triangle BAC$, it is denoted by $\mathrm{lS}\,\triangle BAC$.
- Let AB and AC be two integer segments, then the value
$$\mathrm{lsin}\,\angle BAC = \frac{\mathrm{lS}\,\triangle ABC}{\mathrm{l}\ell(AB)\,\mathrm{l}\ell(AC)}$$
is the *integer sine* of the angle $\angle BAC$.
- Let ℓ be an integer line and A be some integer point outside ℓ. The *integer distance* between A and ℓ is the index of a sublattice generated all integer vectors starting at A and ending at integer points of ℓ in the lattice $\mathbb{Z}^2$.
- Let ℓ_1 and ℓ_2 be two distinct parallel integer lines. The *integer distance* between then is the integer distance between any integer point of ℓ_1 and the line ℓ_2.

Recall that two sets U and V are integer congruent if there is an integer affine transformation (i.e., an affine integer lattice preserving transformation) that is a bijection between U and V. We write $U \cong V$.

2.4. Sails for angles and their LLS sequences, integer arctangents. In this subsection we discuss the classical geometry of continued fractions. We start with the following definition.

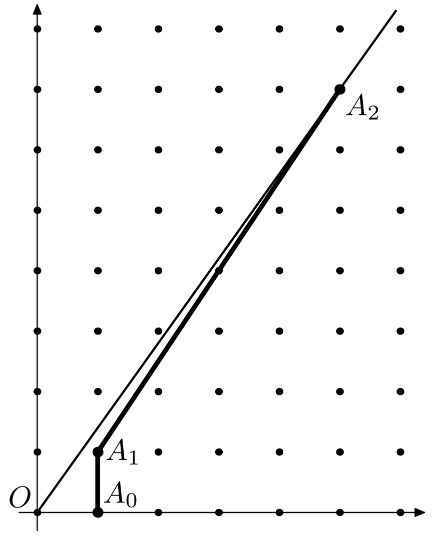

FIGURE 2.1. The sail for an angle.

Definition 2.6. Consider the convex hull of all integer points inside a rational angle α except for its vertex. Then the boundary of this convex hull is a broken line. The *sail* of α is the union of all bounded edges of the broken line.

Definition 2.7. For a rational integer angle α with sail $A_0, \ldots, A_{n+1}$, we define the *LLS sequence* of α as the sequence $(a_0, \ldots, a_{2n})$ where

$$a_{2k} = \mathrm{l}\ell(A_kA_{k+1});$$
$$a_{2k-1} = \mathrm{lsin}(\angle A_{k-1}A_kA_{k+1}).$$

We also write $\mathrm{LLS}(\alpha) = (a_0, \ldots, a_{2n})$. We then define the *integer arctangent* of α as the continued fraction expansion $\mathrm{ltan}(\alpha) = [a_0; a_1, \ldots, a_{2n}]$.

We show an example of the sail for the angle with vertices $(1, 0)$, $(0, 0)$, and $(5, 7)$ on Figure 2.1.

Remark 2.8. Our approach is alternative to Hirzebruch–Jung continued fractions developed in [11] and [12].

Remark 2.9. Here LLS is an abbreviation of "lattice length sine". This comes from the fact that the LLS sequence of a sail is precisely the alternating sequence of integer lengths of its line segments and integer sines of the angles between them.

Note that ltan takes all rational values greater than or equal to 1. In fact, integer tangent is a complete invariant of integer rational angles ([18, Theorem 4.11]). There is a natural way to define the integer arctangent, it is very similar to the Euclidean case.

Definition 2.10. Let $m \geq n$ be two positive integers that are relatively prime. The *integer arctangent* of m/n is the following integer angle

$$\text{larctan}\,\frac{m}{n} = \angle AOB_{m/n},$$

where $A = (1, 0)$, $O = (0, 0)$, and $B_{m/n} = (n, m)$. (See [18] for further details.)

2.5. Locally convex broken lines and their chord curvature. A *convex polygon* P is the intersection of a finite number of affine half-planes; here we also assume that the affine span of the polygon coincides with $\mathbb{R}^2$ and that the intersection is bounded. A point of P is a *vertex* if it does not belong to some open interval contained in the convex hull of P. By this definition all the angles of convex polygons are greater than 0 and smaller than π.

By the definition, any convex polygon has finitely many vertices. A convex n-gon P is therefore given by its vertices $A_1 \ldots A_n$ ordered anticlockwise starting from some arbitrary vertex A_1 and indexed via residues of n. In particular, we write $A_0 = A_n$ and $A_{n+1} = A_1$.

We say that a rational angle $\angle ABC$ is *positively/negatively oriented* if $\det(BA, BC) > 0$ or respectively $\det(BA, BC) < 0$. In case if A, B, and C are in a line we say that the angle *does not have a natural orientation.*

Definition 2.11. We say that an integer broken line is *locally convex* if all its angles are simultaneously either positively oriented or negatively oriented.

Remark 2.12. The boundary broken line of any convex polygon is locally convex.

Definition 2.13. Consider a locally convex broken line $ABCD$ with no three consecutive points being in a line. We say that the *chord curvature* of $ABCD$ is the following quantity

$$\text{æ}(ABCD) = \text{l}\ell(BC) - \text{sgn}\langle BC, B'C' \rangle \cdot \text{l}\ell(B'C') - 2,$$

where

- the point B' is the integer point of the angle ABC at the unit integer distance to the segment BC which is the closest to the line AB;
- the point C' is the integer point of the angle BCD at the unit integer distance to the segment BC which is the closest to the line CD;

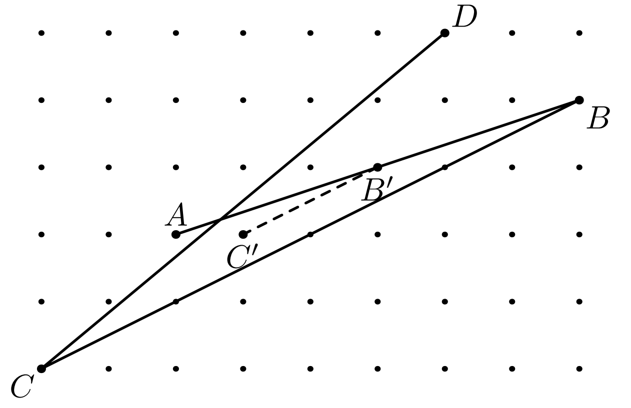

FIGURE 2.2. The broken line $ABCD$ and its points B' and C'.

- the value $\operatorname{sgn}\langle BC, B'C'\rangle$ is defined as follows:

$$\operatorname{sgn}\langle BC, B'C'\rangle = \begin{cases} 1, & \text{if } BC \text{ and } B'C' \text{ has the same direction;} \\ 0, & \text{if } B' = C'; \\ -1, & \text{if } B'C' \text{ has the opposite direction to } BC. \end{cases}$$

Remark 2.14. In the formula defining the chord curvature we subtract two in order to get the simplest expressions in Theorem 3.8. Currently we do not know any other defining property for determining the constant that is subtracted.

Example 2.15. Let us consider the broken line $ABCD$ with points

$$A = (2,2), \qquad B = (8,4), \qquad C = (0,0), \quad \text{and} \quad D = (6,5)$$

(see Figure 2.2). Then $B' = (5,3)$ and $C' = (3,2)$. Thus $\mathrm{l}\ell(BC) = 4$ and $\mathrm{l}\ell(B'C') = 1$ The vector $B'C'$ has the same direction with the vector BC, and hence $\operatorname{sgn}\langle BC, B'C'\rangle = 1$. We have

$$æ(ABCD) = 4 - 1 \cdot 1 - 2 = 1.$$

Let us finally give the definition of chord curvature for broken lines on n vertices.

Definition 2.16. Let $A_1 \ldots A_n$ be a locally convex broken line. We say that the *chord curvature* at an edge A_iA_{i+1} (where $2 \le i \le n-2$) is the chord curvature of $A_{i-1}A_iA_{i+1}A_{i+2}$.

For an arbitrary integer broken line we set the cord curvature for each triple of consecutive edges. Note that the chord curvature is an integer affine invariant of an integer broken.

2.6. Angle-curvature sequences for locally convex broken lines and convex polygons. Let us now define a lattice invariant that will be playing the leading role in our main statements.

Definition 2.17. Let $A_0A_1\ldots A_nA_{n+1}$ be a locally convex broken line. Set

$$\begin{aligned}\alpha_i &= \operatorname{larctan}(\angle A_{i-1}A_iA_{i+1}), &&\text{for } i=1,\ldots,n;\\ \text{æ}_i &= \text{æ}(A_{i-1}A_iA_{i+1}A_{i+2}), &&\text{for } i=1,\ldots,n-1.\end{aligned}$$

We say that the sequence

$$\mathcal{S}=(\alpha_1,\text{æ}_1,\ldots,\alpha_{n-1},\text{æ}_{n-1},\alpha_n)$$

is the *angle-curvature sequence* for the broken line.

Definition 2.18. Let $A_1\ldots A_n$ be a locally convex closed broken line. Set

$$\begin{aligned}\alpha_i &= \operatorname{larctan}(\angle A_{i-1}A_iA_{i+1}), &&\text{for } i=1,\ldots,n;\\ \text{æ}_i &= \text{æ}(A_{i-1}A_iA_{i+1}A_{i+2}), &&\text{for } i=1,\ldots,n.\end{aligned}$$

We say that the sequence

$$\mathcal{S}=(\alpha_1,\text{æ}_1,\ldots,\alpha_{n-1},\text{æ}_{n-1},\alpha_n,\text{æ}_n)$$

is the *angle-curvature sequence* for the broken line.

Remark 2.19. In case if we do not fix a starting point of the closed broken line, the corresponding angle-curvature sequence is considered to by cyclic.

Similar to triangles we give the following criterion of integer congruence of integer broken lines.

Proposition 2.20. *Let two locally convex broken lines* (*including the ones bounding convex polygons*) *be integer congruent then their angle-curvature sequences coincide.* □

Remark 2.21. We use the term “integer congruency” to underline that we consider the integer affine transformations (and not the Euclidean ones).

2.7. Discussion on integer angle-side-curvature-angle rule. From Euclidean geometry we know the classical *ASA* (*angle-side-angle*) *rule*: If two pairs of angles of two triangles are equal, and the included sides are equal, then these triangles are integer congruent.

It turns out that this rule is not sufficient for lattice geometry. Let us illustrate this with the following example

Example 2.22. Let $A=(0,0)$, $B=(2,0)$, $C=(1,1)$, $C'=(0,2)$. Consider triangles $\triangle ABC$ and $\triangle ABC'$. Then

$$\angle BAC \cong \angle BAC' \cong \angle ABC \cong \angle ABC' \cong \operatorname{larctan} 1$$

and both triangles share the same segment ABC. However their lattice areas are

$$\mathrm{lS}(ABC) = 2 \quad \text{and}\, \mathrm{lS}(ABC') = 4,$$

and hence these triangles are not integer congruent to each other.

The notion of chord curvature providing us a new refined rule.

Proposition 2.23. *Two triangles $\triangle ABC$ and $\triangle A'B'C'$ are integer congruent* (*preserving the order of points*) *if and only if the following* integer angle-side-curvature-angle rule (*or* ASCA rule *for short*) *holds:*

$$\angle ABC \cong \angle A'B'C', \quad \angle BAC \cong \angle B'A'C',$$
$$\mathrm{l}\ell(AB) = \mathrm{l}\ell(A'B'), \quad \text{æ}(CABC) = \text{æ}(C'A'B'C').$$

Proof. Let all the ASCA rule condition hold. Consider the transformation sending the angle $\angle C'A'B'$ to the angle $\angle CAB$. Here the images of B' and C' are some points B'' and C'' Since $\mathrm{l}\ell(AB) = \mathrm{l}\ell(A'B') = \mathrm{l}\ell(AB'')$, we have $B'' = B$.

Since $\text{æ}(C''AB''C'') = \text{æ}(C'A'B'C') = \text{æ}(CABC)$ the first edges of the sails of $\angle ABC''$ and $\angle ABC$ have the same direction. Since $\angle BAC'' \cong \angle B'A'C' \cong \angle BAC$, the segment AB is a common edge for the triangles $\triangle ABC''$ and $\triangle ABC''$, and the sails for $\angle ABC''$ and $\angle ABC$ have the same direction, we get that the sails for $\angle ABC''$ and $\angle ABC$ coincide. This implies that the line BC coincides with the line BC''.

The lines AC and AC'' coincide by the construction and the lines BC coincides with the line BC'' from the above. Hence $C = C''$. Therefore, the triangles $\triangle ABC$ and $\triangle A'B'C'$ are integer congruent.

Conversely, if the triangles $\triangle ABC$ and $\triangle A'B'C'$ are integer congruent, then all the listed identities in the ASCA rule hold, since the corresponding quantities are lattice invariants. □

3. Classification of the angles for convex lattice polygons

In this subsection, we formulate the main results of this paper. The proofs are provided later in Section 5.

3.1. Solution to IKEA problem.

We start with the following notation.

Definition 3.1. For an angle-curvature sequence

$$\mathcal{S} = (\alpha_1, \text{æ}_1, \ldots, \alpha_{n-1}, \text{æ}_{n-1}, \alpha_n, \text{æ}_n)$$

we set $\mathcal{S}_j^k$ to be the subsequence $(\alpha_j, \text{æ}_j, \ldots, \alpha_{k-1}, \text{æ}_{k-1}, \alpha_k)$. We then write

$$\mathrm{LLS}(\mathcal{S}_j^k) = \mathrm{LLS}(\alpha_j) \circ (\text{æ}_j) \circ \ldots \circ \mathrm{LLS}(\alpha_{k-1}) \circ (\text{æ}_{k-1}) \circ \mathrm{LLS}(\alpha_k).$$

Definition 3.2. We say an integer sequence *changes sign n times* if after removing all zero elements it contains exactly n pairs of consequent elements with opposite signs.

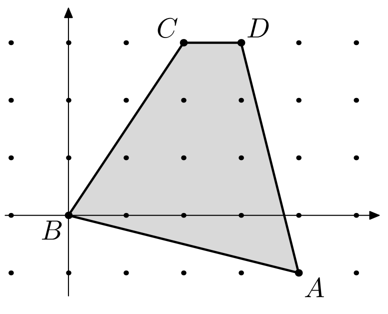

Figure 3.1. The quadrangle $ABCD$.

We are ready to formulate the first main result of the paper.

Theorem 3.3. *Consider the set of rational angles $\alpha_1, \ldots, \alpha_n$ and the integers $æ_1, \ldots, æ_n$. Then there exists a convex n-gon with the prescribed angle-curvature sequence,*

$$\mathcal{S} = (\alpha_1, æ_1, \ldots, \alpha_{n-1}\, æ_{n-1}, \alpha_n, æ_n),$$

if and only if the following conditions hold:

- $K(\mathrm{LLS}(\mathcal{S}_1^n)) = 0$;
- $æ_n = -\left\lfloor \frac{K(\mathrm{LLS}(\mathcal{S}_2^n)\circ(1))}{K(\mathrm{LLS}(\mathcal{S}_2^n))} \right\rfloor$;
- *The sequence $(K(\mathrm{LLS}(\mathcal{S}_1^j)))_{j=1}^n$ changes the sign $n-3$ times.*

Remark 3.4. Once the last condition is removed, we have a similar statement for locally convex closed broken lines.

Remark 3.5. Practically, one may use continued fractions in order to compute the values of continuants. Informally speaking, the continuant of a sequence coincides with the numerator of the continued fraction for the same sequence. An important rule here is to keep the denominators (without cancelling their factors with the factors of the numerators). Let us illustrate this with a sample computation of $K(-1, 2, -3)$. We have:

$$[-1; 2 : -3] = -1 + \frac{1}{2 + \frac{1}{-3}} = -1 + \frac{1}{\frac{-6}{-3} + \frac{1}{-3}} = -1 + \frac{-3}{-5} = \frac{5}{-5} + \frac{-3}{-5} = +\frac{2}{-5}.$$

Hence $K(-1, 2, -3) = 2$.

Let us supplement Theorem 3.3 with the following example.

Example 3.6. Consider a quadrangle with vertices $A = (4, -1)$, $B = (0, 0)$, $C = (2, 3)$, and $D = (3, 3)$ as on Figure 3.1. Direct computations show that the angle-curvature sequence for this quadrangle is as follows:

$$\mathcal{S} = \Big(\text{larctan}([1;3:1:1:1]), -1, \text{larctan}([3]), -2, \\ \text{larctan}([1;2,1]), -1, \text{larctan}([3;1:3]), -1\Big).$$

Let us check the first condition of Theorem 3.3. Indeed we have

$$K(\text{LLS}(\mathcal{S}_1^4)) = K(1,3,1,1,1,-1,3,-2,1,2,1,-1,3,1,3) = 0.$$

The second condition is also true:

$$\begin{aligned} æ_4 = -1 &= -\frac{17}{14} \\ &= -\left\lfloor \frac{K(3,-2,1,2,1,-1,3,1,3,1)}{K(3,-2,1,2,1,-1,3,1,3)} \right\rfloor = \left\lfloor \frac{K(\text{LLS}(\mathcal{S}_2^4) \circ (1))}{K(\text{LLS}(\mathcal{S}_2^4))} \right\rfloor. \end{aligned}$$

For the last condition the corresponding sequence of continuants is as follows:

$$\begin{aligned} K(\text{LLS}(\mathcal{S}_1^1)) &= K(1,3,1,1,1) = 14; \\ K(\text{LLS}(\mathcal{S}_1^2)) &= K(1,3,1,1,1,-1,3) = -1; \\ K(\text{LLS}(\mathcal{S}_1^3)) &= K(1,3,1,1,1,-1,3,-2,1,2,1) = -15; \\ K(\text{LLS}(\mathcal{S}_1^4)) &= K(1,3,1,1,1,-1,3,-2,1,2,1,-1,3,1,3) = 0. \end{aligned}$$

We have a sequence that changes the sign once, exactly $n-3=4-3=1$ times, and thus the last condition also holds.

3.2. Explicit construction of the last entry in the angle-curvature sequence. Let us fix some notation and definitions required for the next theorem. Let S be some finite sequence. We write S^t for the reversed sequence, and we write $-S$ for the sequence with negated terms.

Definition 3.7. Let $(a_0, \dots, a_n)$ be an arbitrary sequence of integers. Set

$$\angle(a_0, \dots, a_n) = \angle AOB,$$

where $A=(1,0)$, $O=(0,0)$, and $B = \big(K(a_1, \dots, a_{2n}), K(a_0, a_1, \dots, a_{2n})\big)$.

Below is the second main result of the paper.

Theorem 3.8. *Consider arbitrary rational angles $\alpha_1, \dots, \alpha_n$ and integers $æ_1, \dots, æ_{n-1}$ where $n \geq 2$. Assume that*

$$\text{LLS}(\alpha_1, æ_1, \dots, æ_{n-1}, \alpha_n) \neq 0.$$

Then there exists a unique locally convex $(n+1)$-gon whose angle-curvature sequence is

$$\mathcal{S} = (\alpha_1, æ_1, \dots, , \alpha_{n-1}\, æ_{n-1}, \alpha_n, x, \beta, y),$$

where the integers x and y and an the rational angle β are defined as follows:

$$x = -\left\lfloor \frac{K(U \circ (1))}{K(U)} \right\rfloor, \qquad \beta \cong \angle(\,-U^t), \qquad y = -\left\lfloor \frac{K(V \circ (1))}{K(V)} \right\rfloor,$$

where

$$\begin{aligned} U &= \mathrm{LLS}(\mathcal{S}_1^n) = \mathrm{LLS}(\alpha_1) \circ (æ_1) \circ \ldots \circ \mathrm{LLS}(\alpha_{n-1}) \circ (æ_{n-1}) \circ \mathrm{LLS}(\alpha_n); \\ V &= \mathrm{LLS}(\mathcal{S}_2^{n+1}) = \mathrm{LLS}(\alpha_2) \circ (æ_2) \circ \ldots \circ \mathrm{LLS}(\alpha_{n-1}) \circ (æ_{n-1}) \circ \mathrm{LLS}(\alpha_n) \\ &\qquad \circ (x) \circ \mathrm{LLS}(\beta). \end{aligned}$$

Remark 3.9. Note that

$$y = \left\lfloor \frac{K(-U^t \circ (-1))}{K(-U^t)} \right\rfloor$$

in the notation of the above theorem.

Example 3.10. Consider three angles α_1, α_2 and α_3 with LLS sequences $(1,3,1,1,1)$, (3), and $(1,2,1)$. Let also $æ_1 = -1$ and $æ_2 = -2$. Then

$$\begin{aligned} U &= \mathrm{LLS}(\alpha_1) \circ (æ_1) \circ \mathrm{LLS}(\alpha_2) \circ (æ_2) \circ \mathrm{LLS}(\alpha_3) \\ &= (1,3,1,1,1) \circ (-1) \circ (3) \circ (-2) \circ (1,2,1) \\ &= (1,3,1,1,1,-1,3,-2,1,2,1) \end{aligned}$$

and hence

$$x = -\left\lfloor \frac{K(U \circ (1))}{K(U)} \right\rfloor = -\left\lfloor \frac{K(1,3,1,1,1,-1,3,-2,1,2,1,1)}{K(1,3,1,1,1,-1,3,-2,1,2,1)} \right\rfloor = -\left\lfloor \frac{-26}{-15} \right\rfloor = -1.$$

Further we have

$$-U^t = (-1,-2,-1,2,-3,1,-1,-1,-1,-3,-1).$$

Now we compute the continued fraction corresponding to the last sequence:

$$[-1; -2 : -1 : 2 : -3 : 1 : -1 : -1 : -1 : -3 : -1] = \frac{15}{-11}$$

(here we take care of the signs for continuants in the fraction). Then β is integer congruent to the angle with vertices

$$(1,0), \quad (0,0), \quad \text{and} \quad (-11,15).$$

In terms of arctangents we have

$$\beta \cong \mathrm{larctan}\left(\frac{15}{-11 (\mathrm{mod}\, 15)}\right) = \mathrm{larctan}\left(\frac{15}{4}\right).$$

Since $15/4 = [3;1;3]$, we get $\mathrm{LLS}(\beta) = (3,1,3)$. Finally,

$$V = \mathrm{LLS}(\alpha_2) \circ (æ_2) \circ \mathrm{LLS}(\alpha_3) \circ (x) \circ \mathrm{LLS}(\beta) = (3,-2,1,2,1,-1,3,1,3),$$

and hence

$$y = -\left\lfloor \frac{K(V \circ (1))}{K(V)} \right\rfloor = -\left\lfloor \frac{K(3,-2,1,2,1,-1,3,1,3,1)}{K(3,-2,1,2,1,-1,3,1,3)} \right\rfloor = -\left\lfloor \frac{-17}{-14} \right\rfloor = -1.$$

(This example correspond to the quadrangle of Example 3.6, the quadrangle is shown on Figure 3.1 above.)

4. Further tools needed for the proof

This subsection contains some extra definitions, notions, and statements that are used in the proofs of the next section.

4.1. Sail diagrams for broken lines. Let us generalise the notion of the sail for an integer angle to the case of broken lines with integer vertices.

Definition 4.1. The *sail diagram* of a broken line (closed or not closed) with integer vertices is the broken line obtain by the sails of the consecutive angles of the broken line shifted to the origin (in composition with the central symmetry for all even ones).

The vertices of the sail diagram corresponding to the edges of the angles are called *edge vertices*.

Remark 4.2. The sail diagram for a broken line coincides with the sail diagram of the sum of its interior angles corresponding to integer parallel transform of these angles to the origin and symmetries about the origin for angles with even numbers.

Remark 4.3. In case of a convex polygon with even number of vertices its sail diagram is a closed broken line. If the number of vertices is odd, then the starting and the end points of the sail diagram are two points symmetric with respect to the origin.

Example 4.4. Let us consider a pentagon (see on Figure 4.1, Left) with vertices

$$(8,0), \quad (0,0), \quad (2,3), \quad (3,4), \quad \text{and} \quad (5,3).$$

Then its angle-curvature sequence is

$$\Big(\operatorname{larctan}(3/2), -2, \operatorname{larctan}(1), -4, \operatorname{larctan}(3), -2, \operatorname{larctan}(1), -3, \operatorname{larctan}(1), 0\Big).$$

The corresponding sail diagram (see on Figure 4.1, Right) has vertices

$$(1,0), \quad (1,1), \quad (2,3), \quad (-1,-1), \quad (2,-1), \quad (-1,1), \quad \text{and} \quad (-1,0).$$

All these vertices except $(1,1)$ are edge vertices.

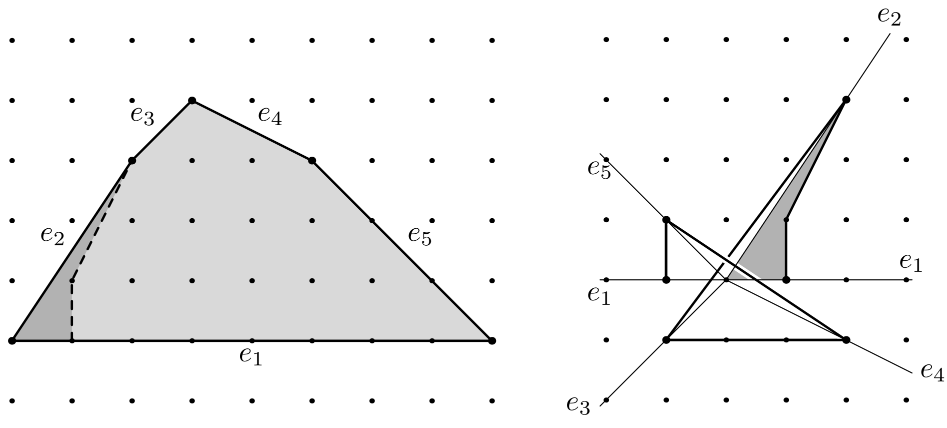

FIGURE 4.1. A pentagon with marked (on the left) edges and its sail diagram (on the right). We indicate one of the angles and the corresponding angle of the diagram with dark grey.

4.2. Vortex broken lines, their tangents and LLS sequences. Let us give a formal definition of a broken line bending counterclockwise with respect to some point.

Definition 4.5. We say that a broken line $A_1 \dots A_n$ is a *vortex broken line about O* if

$$\det(OA_i, OA_{i+1}) > 0 \qquad \text{for } i = 1, \dots, n-1.$$

It turns out that the notion of LLS sequences is naturally extended to vortex broken lines (for further details see Chapter 15 of [18]).

Definition 4.6. For some integer vortex broken line $A_0 \dots A_m$ we define the *LLS sequence* of the broken line as the sequence $a_0, \dots, a_{2n}$ where

$$a_{2k} = \det(OA_k, OA_{k+1}) = \mathrm{l}\ell(A_kA_{k+1}) \quad \text{for } k = 0, 1, \dots, n;$$
$$a_{2k-1} = \frac{\det(A_{k+1}A_k, A_{k+1}A_{k+2})}{a_{2k-1}a_{2k+1}} \qquad \text{for } k = 1, 2, \dots, n.$$

We also write $\mathrm{LLS}(A_0 \dots A_m) = (a_0, \dots, a_{2n})$.

Let us finally recall the following important expression for the vertex coordinates of vortex broken lines (in fact the original statement is for a broader selection of broken lines).

Theorem 4.7 ([18, Theorem 15.10])**.** *Consider a vortex broken line $A_0 \dots A_n$ about the origin with LLS sequence*

$$(a_0, a_1, \dots, a_{2n-2}).$$

Let also $A_0 = (1, 0)$ *and* $A_1 = (1, a_0)$*. Then*

$$A_i = \big(K(a_1, \dots, a_{2i-2}), K(a_0, a_1, \dots, a_{2i-2})\big) \quad \textit{for } i = 1, \dots, n.$$

Remark 4.8. The LLS sequence is the complete invariant of integer congruence types of integer winding broken lines. Namely, two integer winding broken lines are integer congruent if and only if they have the same LLS sequence. In addition, an arbitrary sequence of odd length of integers with positive odd elements is the LLS sequence for some integer winding broken line.

Remark 4.9. In accordance with Definition 3.7, we have

$$\angle(a_0, a_1, \dots, a_{2n-2}) \cong \angle A_0 O A_n.$$

We conclude this section with the following general proposition.

Proposition 4.10. *Any sail diagram is a vortex broken line about the origin. In addition, all the edges of the sail diagram at the unit distance to the origin.*

Proof. Note that the sail for any integer angle is a vortex broken line with edges at the unit distance to the origin. Since the sail diagram is the union of several sails, it also satisfies the conditions of the proposition. □

4.3. Winding number of sail diagrams and its properties. Denote by $\mu(\varphi)$ the Euclidean angular measure of the angle φ.

Definition 4.11. The *winding number* of a vortex broken line $A_0 \dots A_n$ about a point O is the following number

$$\omega(A_0 \dots A_n, O) = \frac{1}{2\pi} \sum_{i=1}^{n} \mu(\angle A_{i-1} O A_i).$$

In general, the winding number is not an invariant of lattice geometry except for the case when it is half an integer. (The last correspond to the projectivisation of the Gauss map to the projective circle, and therefore it is a topological invariant). That is precisely the case of the sail diagrams of convex polygons.

Proposition 4.12. *The winding number of the sail diagram of the convex* n*-gon equals* $n/2 - 1$*.*

Remark 4.13. In particular, the winding number of the sail diagram of a convex polygon is its invariant in integer geometry.

Proof. It is clear that the sum of angles for the sail diagram equals the sum of angles of the n-gon. Namely, it is equivalent to $(n-2)\pi$ and hence the winding number equals $n/2 - 1$. □

Proposition 4.14. *Let $A_0 \ldots A_n$ be a sail diagram for an n-gon with an angle-curvature sequence*

$$\mathcal{S} = (\alpha_1, æ_1, \ldots, \alpha_{n-1}, æ_{n-1}, \alpha_n, æ_n).$$

Then, the number of sign changes for the sequence $(\mathrm{LLS}(\mathcal{S}_1^j))_{j=1}^n$ equals twice the winding number of $A_0 \ldots A_n$ about the origin minus 1. (Here $\mathcal{S}_1^j$ are as in Definition 3.1.)

Proof. Let us first consider a sail diagram whose first two vertices are $A_0 = (1,0)$ and $A_1 = (1, a_0)$.

By Theorem 4.7, the sequence $(\mathrm{LLS}(\mathcal{S}_1^j))_{j=1}^n$ coincides with the sequence of y coordinates of the vertices of the broken line connecting all the edge vertices of the sail diagram. Since the original polygon is convex, this broken line makes precisely $n-2$ half-twists around the origin. Again, due to convexity of the original polygon, we always add angles that are less than π and hence the sequence of y coordinates changes sign precisely $n-3$ times. Now the proof is concluded by Proposition 4.12.

Let us now study the case of general sail diagrams. First of all, note that such sail diagrams are integer congruent to some of the diagrams considered above. Secondly, both the winding number and the LLS sequence (and hence the number of sign changes) are invariants of integer geometry. This concludes the proof in the general case. □

Remark 4.15 (Cusps of sail diagrams and polygons)**.** We say that the sail diagram has a cusp in edge vertex B_i if the chord curvature $æ_i < 0$. Note that any broken line with only positive numbers in the LLS sequence winds less than π around the origin. Since any n-gon does $n-2$ half twists around the origin starting from any vertex (this means that we forget one of the cusps), the sail diagram has at least $n-1$ cusp. In case of the number of cusps of the sail polyhedron is smaller than $n-1$, the corresponding broken line is still locally convex, however the sum of its angles is smaller than $\pi(n-3)$, and therefore it has self-intersections.

4.4. A few words about special integer points on sail diagrams. Let formulate the following variation of the general classic matrix identity for continuants.

Proposition 4.16. *Consider an arbitrary sequence of numbers $(b_0, \ldots, b_k)$ and set $b_{-1} = 0$. Then the following identity holds:*

$$\begin{pmatrix} K(b_1, \ldots, b_k) \\ K(b_0, \ldots, b_k) \end{pmatrix} = M_k \begin{pmatrix} 1 \\ 0 \end{pmatrix}, \qquad \textit{where} \quad M_k = \prod_{i=0}^{k+1} \begin{pmatrix} 0 & 1 \\ 1 & b_{k-i} \end{pmatrix}.$$

Let us fix some notation. Denote by $B_i(p_i, q_i)$ the edge vertices of the sail diagram. Denote also the next and the previous integer points with respect

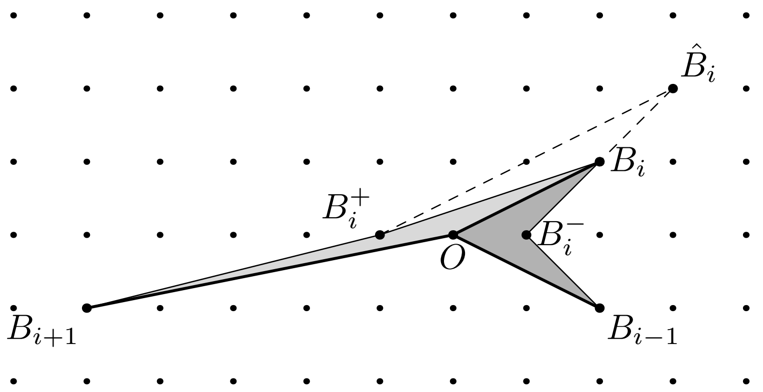

FIGURE 4.2. Definition of points B_i^-, B_i^+, and $\widehat{B}_i$.

to B_i on the sail diagram by B_i^+ and by B_i^- respectively. Let

$$\mathrm{LLS}(\mathcal{S}_1^i) = (b_0, \dots, b_{2s(i)}),$$

and let $b_{2s(i)+1}$ be the next element of the LLS sequence for the sail diagram. (Note that $s(i)$ is the total number of edges in the sails of the first i integer angles.)

From the expression for the LLS sequence of a broken lines we have (see Theorem 15.10 and Remark 15.11 of [18]):

$$B_i = \big(K(b_1, \dots, b_{2s(i)-1}, b_{2s(i)}), K(b_0, \dots, b_{2s(i)-1}, b_{2s(i)})\big).$$

Further for the next and previous integer points with respect B_i we have (see Section 15 and Subsection 9.3 of [18]):

$$\begin{aligned} B_i^- &= \big(K(b_1, \dots, b_{2s(i)-1}, b_{2s(i)}-1), K(b_0, \dots, b_{2s(i)-1}, b_{2s(i)}-1)\big); \\ B_i^+ &= \big(K(b_1, \dots, b_{2s(i)-1}, b_{2s(i)}, b_{2s(i)+1}, 1), \\ &\qquad\qquad K(b_0, \dots, b_{2s(i)-1}, b_{2s(i)}, b_{2s(i)+1}, 1)\big). \end{aligned}$$

Set also

$$\widehat{B}_i = \big(K(b_1, \dots, b_{2s(i)-1}, b_{2s(i)}, 0, 1), K(b_0, \dots, b_{2i-1}, b_{2s(i)}, 0, 1)\big).$$

(See Figure 4.2.)

Proposition 4.17. *The following statements hold:*

(i) $b_{2s(i)+1} = \det(B_iB_i^-, B_iB_i^+)$;
(ii) $b_{2s(i)+1} = æ_i$;
(iii) $\widehat{B}_i = B_i + B_i^- B_i$;
(iv) $b_{2s(i)+1} = \det(B_iB_i^+, B_i\widehat{B}_i)$;
(v) *The points B_i^+ and $\widehat{B}_i$ are in a line parallel to the line OB_i at the unit integer distance to OB_i;*

(vi) *The second coordinate of* $\widehat{B}_i$ *is* $K(\mathrm{LLS}(\mathcal{S}_1^i) \circ (1))$*;*

(vii) *The second coordinate of* B_{n-1}^+ *is in the interval between* 0 *and* $K(\mathrm{LLS}(\mathcal{S}_1^{n-1}))$*. It can take zero extreme value but not the other one.*

Proof. (i). From general theory of continued fractions for broken lines (see e.g. in [14]), the point B_i^- is the last integer point of the last edge of the sail for α_i; and the point B_i^+ is the last integer point of the last edge of the sail for α_{i+1} and hence, by the definition of the LLS sequence we have

$$b_{2s(i)+1} = \frac{\det(B_iB_i^-, B_iB_i^+)}{\mathrm{l}\ell(B_iB_i^-) \cdot \mathrm{l}\ell(B_iB_i^+)} = \frac{\det(B_iB_i^-, B_iB_i^+)}{1 \cdot 1} = \det(B_iB_i^-, B_iB_i^+).$$

(ii). Both b_{2i+1} and $æ_i$ are invariants of integer geometry and hence without loss of generality we restrict ourselves to the case (by changing the lattice coordinates):

$$B_i^- = (b_{2s(i)+1} + 1, -1), \quad B_i = (1, 0), \quad B_i^+ = (0, 1),$$

On the one hand, we have

$$\det(B_iB_i^-, B_iB_i^+) = b_{2s(i)+1}.$$

On the other hand, let us consider the edge A_iA_{i+1} in the polygon for the given sail diagram corresponding to the edge vertex B_i (see Figure 4.3). The edge A_iA_{i+1} is parallel to the x-axes. Without loss of generality, we consider $A_i = (0, 0)$ and $A_{i-1} = (a, 0)$ where $a = \mathrm{l}\ell(A_{i-1}A_i)$. Then, the points A_i' and A_{i-1}' as in Definition 2.13 will be the last and the first integer points on the sails for the angles $\angle A_{i-2}A_{i-1}A_i$ and $\angle A_{i-1}A_iA_{i+1}$ respectively. Hence, they are

$$\begin{aligned} A_{i-1}' &= A_{i-1} - OB_i^- = (a, 0) + (-b_{2s(i)+1} - 1, 1) = (a - b_{2s(i)+1} - 1, 1); \\ A_i' &= A_i + OB_i^+ = (1, 0) + (0, 1) = (1, 1). \end{aligned}$$

Then, by the definition of chord curvature we get

$$\begin{aligned} æ_i &= \mathrm{l}\ell(A_{i-1}A_i) - \mathrm{sgn}\langle A_{i-1}A_i, A_{i-1}'A_i'\rangle\, \mathrm{l}\ell(A_{i-1}'A_i') - 2 \\ &= a - (a - b_{2s(i)+1} - 2) - 2 = b_{2s(i)+1}. \end{aligned}$$

Therefore,

$$æ_i = \det(B_iB_i^-, B_iB_i^+) = b_{2s(i)+1}.$$

(iii). Denote

$$M = \begin{pmatrix} 0 & 1 \\ 1 & b_{2s(i)} - 1 \end{pmatrix} \prod_{j=1}^{2s(i)} \begin{pmatrix} 0 & 1 \\ 1 & b_{2s(i)-j} \end{pmatrix}.$$

Then, by Proposition 4.16, we have

$$B_i^- = M\begin{pmatrix} 1 \\ 0 \end{pmatrix}, \quad B_i = \begin{pmatrix} 0 & 1 \\ 1 & 1 \end{pmatrix}\begin{pmatrix} 0 & 1 \\ 1 & 0 \end{pmatrix} M \begin{pmatrix} 1 \\ 0 \end{pmatrix}, \quad \widehat{B} = \begin{pmatrix} 0 & 1 \\ 1 & 2 \end{pmatrix}\begin{pmatrix} 0 & 1 \\ 1 & 0 \end{pmatrix} M \begin{pmatrix} 1 \\ 0 \end{pmatrix}.$$

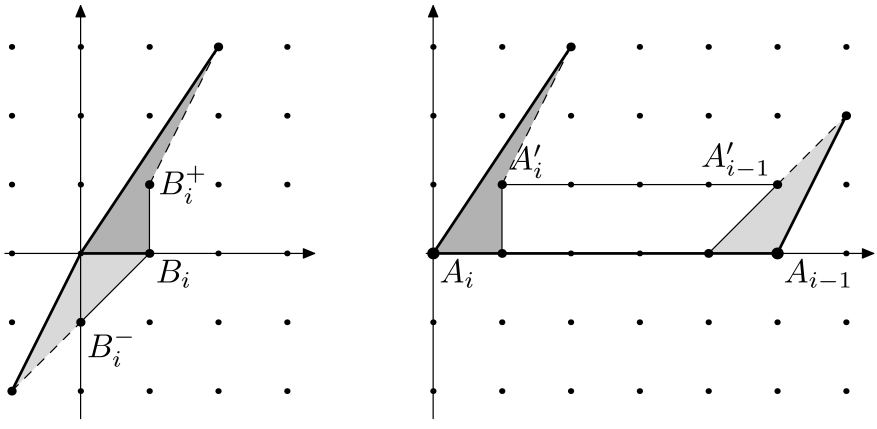

FIGURE 4.3. Two consecutive angles (Left) in the sail diagram and the corresponding edge of the polygon (Right).

Since $M \in \mathrm{GL}(2,\mathbb{Z})$, the statement is equivalent to the statement for the points

$$\begin{pmatrix}1\\0\end{pmatrix}, \quad \begin{pmatrix}0&1\\1&1\end{pmatrix}\begin{pmatrix}0&1\\1&0\end{pmatrix}\begin{pmatrix}1\\0\end{pmatrix}=\begin{pmatrix}1\\1\end{pmatrix}, \quad \begin{pmatrix}0&1\\1&2\end{pmatrix}\begin{pmatrix}0&1\\1&0\end{pmatrix}\begin{pmatrix}1\\0\end{pmatrix}=\begin{pmatrix}1\\2\end{pmatrix},$$

which obviously holds.

(iv). Since $B_iB_i^+ = B_i^-B_i$, the values of the determinants coincide, so we have:

$$b_{2s(i)+1} = \det(B_iB_i^-, B_iB_i^+) = \det(B_iB_i^+, B_i\widehat{B}_i).$$

(v). The points B_i^+ and B_i^- are at unit distance from the segment OB_i since they are the first and the last points of the corresponding sails. They are in different half-planes with respect to the line containing OB_i. By Item (iii), the point $\widehat{B}_i$ is at unit distance to OB_i in the different hyperplane to the point B_i^-. Therefore, the points B_i^+ and $\widehat{B}_i$ are in a line parallel to the line OB_i at the unit integer distance to it.

(vi). The second coordinate of B_i^+ it is equivalent to

$$\begin{aligned}K(b_0,\ldots,b_{2s(i)-1},b_{2s(i)},b_{2s(i)+1},0,1) &= K(b_0,\ldots,b_{2s(i)-1},b_{2s(i)},b_{2s(i)+1},1)\\ &= K(\mathrm{LLS}(\mathcal{S}_1^i)\circ(1)).\end{aligned}$$

(vii). Note that B_i^+ is the first integer point of sail of the angle $\angle B_iOB_0$. Therefore, the second coordinate of B_i^+ has the same sign as B_i (or B_i^+ can be zero), the absolute value of the second coordinate of B_i^+ is smaller than the absolute value of the second coordinate of B_i. This concludes the proof. □

Corollary 4.18. *The LLS sequence of the sail diagram of a convex integer polygon P coincides with the LLS sequence for the angle-curvature sequence of the boundary of P.*

Proof. By construction of the sail diagram, all the elements of the sails of angles coincide with the corresponding elements for the LLS sequences of angles in the angle-curvature.

By Proposition 4.17 (i) and (ii), we have

$$æ_i = \det(B_iB_i^-, B_iB_i^+).$$

The last expression is precisely the expression for the corresponding angle in Definition 4.6 after rescaling the corresponding vectors.

Therefore, the LLS sequence of a the sail diagram coincides with the LLS sequence for the angle-curvature sequence. □

Corollary 4.19. *It holds*

$$æ_{n-1} = -\left\lfloor \frac{K(\mathrm{LLS}(\mathcal{S}_1^{n-1}) \circ (1))}{K(\mathrm{LLS}(\mathcal{S}_1^{n-1}))} \right\rfloor.$$

Proof. By Proposition 4.17 (vi), the numerator of the expression on the right hand side contains the second coordinate of $\widehat{B}_{n-1}$. By construction, the denominator contains the second coordinate of B_{n-1}. Finally, by Proposition 4.17 (vii), the second coordinate of $\widehat{B}_{n-1}^+$ is in the segment $[0, K(\mathrm{LLS}(\mathcal{S}_1^{n-1}))$ excluding the right end.

By Proposition 4.17 (v), the points B_{n-1}^+ and $\widehat{B}_{n-1}$ are in a line that is parallel to OB_i; and the integer distance between this line and the line OB_i equals 1. Therefore, computing the second coordinates we have

$$\det(B_{n-1}B_{n-1}^+, B_{n-1}\widehat{B}_{n-1}) = -\left\lfloor \frac{K(\mathrm{LLS}(\mathcal{S}_1^{n-1}) \circ (1))}{K(\mathrm{LLS}(\mathcal{S}_1^{n-1}))} \right\rfloor.$$

It remains to note that, by Proposition 4.17(iv), it holds

$$\det(B_{n-1}B_{n-1}^+, B_{n-1}\widehat{B}_{n-1}) = æ_{n-1}\,.$$

This concludes the proof. □

5. Proofs of the main results

In this section we conclude the proofs of Theorem 3.3 and Theorem 3.8.

5.1. Proof of Theorem 3.3.

From a polygon to three conditions. Consider a convex n-gon with the angle-curvature sequence $\mathcal{S}$.

Without loss of generality, we may assume that the first two vertices of the corresponding sail diagram are $A_0 = (1,0)$ and $A_1 = (1,a_0)$. First of all, by Corollary 4.18 the LLS sequence of the sail diagram coincides with the LLS sequence for the angle-curvature sequence. Then, by Theorem 4.7, the sequence $(\mathrm{LLS}(\mathcal{S}_1^j))_{j=1}^n$ coincides with the sequence of y coordinates of the broken line connecting all the edge vertices of the sail diagram. Since the last point of the sail diagram is $((-1)^n, 0)$, the first condition is immediate.

The second condition follows directly from Corollary 4.19 (after shifting all the indices by 1).

The last condition follows directly from Proposition 4.14.

From three conditions to a polygon. Let us now construct a polygon with integer angles integer congruent to given ones: $\alpha_1, \ldots, \alpha_n$ and with corresponding chord curvatures $æ_1, \ldots, æ_n$ satisfying all the conditions of Theorem 3.3.

Let us write the angle-curvature sequence

$$\mathcal{S} = (\alpha_1, æ_1, \ldots, \alpha_{n-1}, æ_{n-1}, \alpha_n)$$

and the corresponding LLS-sequence for it. Starting with vertices $(1,0)$ and $(1,a)$, we construct the broken line with vertices whose coordinates are defined from this LLS-sequence by the formulae of Theorem 4.7. By the first and the third conditions, this broken line has the second endpoint at the line $y=0$ and its winding number is $n/2-1$.

So we have constructed a sail diagram for our prescribed collection of angles and cord curvatures.

Let us find one of the integer polygons with a given sail diagram. First, we find an n-gon whose angles are shifted by arbitrary real vectors (here we take centrally symmetric for even angles); we omit the proof of this classical statement on Euclidean geometry here. Since all vectors are proportional to integer vectors, there exists a small parallel perturbation of this n-gon, that has rational coordinates. Finally, we arrive to an integer n-gon by scaling the rational polygon (multiplying by all denominators of rational coordinates of all vertices).

By the above construction the angles of the obtained polygon are shifted angles (we take centrally symmetric for even angles) of the original sail diagram. Therefore, by the definition, the sail diagram of the obtained polygon is precisely the original sail diagram.

It remains to note that the LLS-sequence of this sail diagram coincide with the LLS-sequence for the angle-curvature of the boundary of the n-gon by Proposition 4.14. This completes the proof. □

Remark 5.1. The construction used in the proof suggests that there are infinitely many distinct integer types of polytopes with a given angle-curvature sequence. Note also that two n-gons whose boundaries have the same angle-curvature sequence are *parallel to each other* (after an integer-affine transformation of one of them), namely the sides of the first n-gon are parallel to the corresponding sides of the second n-gone. The situation here is similar to the Euclidean case.

5.2. Proof of Theorem 3.8. The expressions for x and y follow directly from Corollary 4.19.

The expression for β is tautological. Indeed the sail diagram B defining β has the LLS sequence $\mathrm{LLS}(\mathcal{S}_1^n)$. Then, let us show that $\beta \cong \angle(- U^t)$ where $U = \mathrm{LLS}(\mathcal{S}_1^n)$.

Consider the angle $-\beta$ (this is the angle symmetric to the angle β about the x-axis with the first edge at the origin). Then we take the broken line B' symmetric about the x-axis to the broken line B. By Definition 4.6, the LLS-sequence for B is precisely $-U$. Hence by Theorem 4.7

$$-\beta \cong \angle(B') = \angle(-B) \cong \angle(-U).$$

Finally, we have

$$\beta \cong -\beta^t \cong \big(\angle(-U)\big)^t = \angle(-U^t)$$

as it is stated in the theorem. □

6. A few words on the multidimensional case

We conclude this paper with a small discussion of the open IKEA problem in the multidimensional case.

Problem 2 (IKEA problem in higher dimensions)**.** Classify all angles in lattice convex polyhedra in dimensions greater than 2.

How to generalize the statements of Theorems 3.3 and 3.8? In order to approach this problem one might consider some multidimensional continued fractions.

There are at least two competing theories of multidimensional continued fractions. The first is based on geometry of lattices. Here again we have at least two different version of continued fractions that may be used here: Klein polyhedra [1, 18, 22, 23] and Minkovski–Voronoi polyhedra [20, 26, 27, 33]. The second approach is based on the algorithmic theory of multidimensional continued fractions [19, 31]. (Some further problems on geometric continued fractions are collected in [17].) The problem is open in all the above settings. The progress in it will contribute to the study of singularities of toric varieties, see, e.g. [32].

Finally, we would like to mention a recent progress in the study of lattice trigonometry for cones in higher dimensions in [5].

Acknowledgments. We are grateful to the unknown reviewer for helpful comments and suggestions.

References

[1] V. I. Arnold, "Statistics of integral convex polygons", *Funct. Anal. Appl.* **14** (1980), p. 79-81, Russian version in *Funkts. Anal. Prilozh.* **14(2)** (1980), p. 1-3.

[2] ———, *Continued fractions*, Moscow Center of Continuous Mathematical Education, 2002, in Russian.

[3] I. Bárány & A. M. Vershik, "On the number of convex lattice polytopes", *Geom. Funct. Anal.* **2** (1992), no. 4, p. 381-393.

[4] M. Beck & S. Robins, *Computing the continuous discretely. Integer-point enumeration in polyhedra*, Undergraduate Texts in Mathematics, Springer, 2007, xviii+226 pages.

[5] J. Blackman, J. Dolan & O. Karpenkov, "Multidimensional integer trigonometry", *Commun. Math.* **31** (2023), no. 2, p. 1-26.

[6] W. Castryck & F. Cools, "The lattice size of a lattice polygon", *J. Comb. Theory* **136** (2015), p. 64-95.

[7] F. Eisenbrand & S. Laue, "A linear algorithm for integer programming in the plane", *Math. Program.* **102** (2005), no. 2, p. 249-259.

[8] F. Eisenbrand & G. Rote, "Fast 2-variable integer programming", in *Integer programming and combinatorial optimization (Utrecht, 2001)*, Lecture Notes in Computer Science, vol. 2081, Springer, 2001, p. 78-89.

[9] A. Harrison, J. Soprunova & P. Tierney, "Lattice size of plane convex bodies", *SIAM J. Discrete Math.* **36** (2022), no. 1, p. 92-102.

[10] M. Henk, S. Kuhlmann & R. Weismantel, "On lattice width of lattice-free polyhedra and height of Hilbert bases", *SIAM J. Discrete Math.* **36** (2022), no. 3, p. 1918-1942.

[11] F. Hirzebruch, "Über vierdimensionale Riemannsche Flächen mehrdeutiger analytischer Funktionen von zwei komplexen Veränderlichen", *Math. Ann.* **126** (1953), p. 1-22.

[12] H. W. E. Jung, "Darstellung der Funktionen eines algebraischen Körpers zweier unabhängigen Veränderlichen x, y in der Umgebung einer Stelle $x = a$, $y = b$", *J. für Math.* **133** (1908), p. 289-314.

[13] O. Karpenkov, "On an invariant Möbius measure and the Gauss–Kuz'min face distribution", *Tr. Mat. Inst. Steklova* **258** (2007), p. 74-86, Russian version in *Tr. Mat. Inst. Steklova* **258** (2007), p. 79-92.

[14] ———, "Elementary notions of lattice trigonometry", *Math. Scand.* **102** (2008), no. 2, p. 161-205.

[15] ———, "On irrational lattice angles", *Funct. Anal. Other Math.* **2** (2009), no. 2-4, p. 221-239.

[16] ———, "Continued fractions and the second Kepler law", *Manuscr. Math.* **134** (2011), no. 1-2, p. 157-169.

[17] ———, "Open problems in geometry of continued fractions", 2017, `https://arxiv.org/abs/1712.01450`.

[18] ———, *Geometry of Continued Fractions*, 2nd ed., Algorithms and Computation in Mathematics, vol. 26, Springer, 2022, xx+451 pages.

[19] ———, "On Hermite's problem, Jacobi–Perron type algorithms, and Dirichlet groups", *Acta Arith.* **203** (2022), no. 1, p. 27-48.

[20] O. Karpenkov & A. Ustinov, "Geometry and combinatoric of Minkowski-Voronoi 3-dimensional continued fractions", *J. Number Theory* **176** (2017), p. 375-419.

[21] A. Y. Khinchin, *Continued fractions*, FISMATGIS, 1961.

[22] F. Klein, "Ueber eine geometrische Auffassung der gewöhnliche Kettenbruchentwicklung", *Gött. Nachr.* **3** (1895), p. 352-357.

[23] ———, "Sur une représentation géométrique de développement en fraction continue ordinaire", *Nouv. Ann.* **15** (1896), no. 3, p. 327-331.

[24] M. L. Kontsevich & Y. M. Suhov, "Statistics of Klein polyhedra and multidimensional continued fractions", in *Pseudoperiodic topology*, Translations. Series 2. American Mathematical Society, vol. 197, American Mathematical Society, 1999, p. 9-27.

[25] H. W. Lenstra, Jr., "Integer programming with a fixed number of variables", *Math. Oper. Res.* **8** (1983), no. 4, p. 538-548.

[26] H. Minkowski, "Généralisation de la théorie des fractions continues", *Ann. Sci. Éc. Norm. Supér.* **13** (1896), no. 3, p. 41-60.

[27] ———, *Gesammelte Abhandlungen*, AMS Chelsea Publishing, 1967.

[28] F. Mohammadi & X. Wu, "Rational tensegrities through the lens of toric geometry", 2022, https://arxiv.org/abs/2212.13189.

[29] R. Morrison & A. K. Tewari, "Convex lattice polygons with all lattice points visible", *Discrete Math.* **344** (2021), no. 1, article no. 112161 (19 pages).

[30] J. Schicho, "Simplification of surface parametrizations — a lattice polygon approach", *J. Symb. Comput.* **36** (2003), no. 3-4, p. 535-554, International Symposium on Symbolic and Algebraic Computation (ISSAC'2002) (Lille).

[31] F. Schweiger, *Multidimensional continued fractions*, Oxford Science Publications, Oxford University Press, 2000, viii+234 pages.

[32] H. Tsuchihashi, "Higher-dimensional analogues of periodic continued fractions and cusp singularities", *Tôhoku Math. J. (2)* **35** (1983), p. 607-639.

[33] G. Voronoi, "A generalization of the algorithm of continued fractions", PhD Thesis, Warsaw, 1896, in Russian.

James Dolan
Department of Mathematical Sciences, University of Liverpool
Mathematical Sciences Building
Liverpool, L69 7ZL, United Kingdom
E-mail: james.dolan@liverpool.ac.uk
URL: https://pcwww.liv.ac.uk/~jgd511/

Oleg Karpenkov
Department of Mathematical Sciences, University of Liverpool
Mathematical Sciences Building
Liverpool, L69 7ZL, United Kingdom
E-mail: karpenk@liverpool.ac.uk
URL: https://pcwww.liv.ac.uk/~karpenk/